Functional Conformation Changes in the TF_1-ATPase β Subunit Probed by 12 Tyrosine Residues

Hiromasa Yagi,* Kaeko Tozawa,* Nobuaki Sekino,* Tomoyuki Iwabuchi,* Masasuke Yoshida,# and Hideo Akutsu*

*Department of Chemistry and Biotechnology, Faculty of Engineering, Yokohama National University, Yokohama 240-8501, and #Research Laboratory of Resources Utilization, Tokyo Institute of Technology, Yokohama 226-0026, Japan

ABSTRACT The effect of nucleotide binding on the structure of the F_1-ATPase β subunit from thermophilic bacillus PS-3 ($TF_1\beta$) was investigated by monitoring the NMR signals of the 12 tyrosine residues. The 3,5-proton resonances of 12 tyrosine residues could be observed for the specifically deuterated β subunit. The assignment of 3,5-proton resonances of all of the tyrosine residues was accomplished using 14 mutant proteins, in each of which one or two tyrosine residues were replaced by phenylalanine. Binding of Mg·ATP induced an upfield shift of Tyr^{341} resonance, suggesting that their aromatic rings are stacked to each other. Besides Tyr^{341}, the signal shift observed on Mg·ATP binding was restricted to the resonances of Tyr^{148}, Tyr^{199}, Tyr^{238}, and Tyr^{307}, suggesting that Mg·ATP induces a conformational change in the hinge region. This can be correlated to the change from the open to closed conformations as implicated in the crystal structure. Mg·ADP induced a similar but distinctly different conformational change. Therefore, the intrinsic conformational change in the β subunit induced by the nucleotide binding is proposed to be one of the essential driving forces for the F_1 rotation. Reconstitution experiments showed that Tyr^{277}, one of the four conserved tyrosines, is essential to the formation of the $\alpha_3\beta_3\gamma$ complex.

INTRODUCTION

The H^+-translocating ATP synthase is a multisubunit complex that is composed of a soluble catalytic part (F_1) and a membranous proton-conducting part (F_O). The F_1 portion (F_1-ATPase) has five kinds of subunits with a stoichiometry of $\alpha_3\beta_3\gamma_1\delta_1\epsilon_1$, and the molecular mass is ~380 kDa. The crystal structure of F_1 from bovine heart mitochondria (MF_1) provided us with information at atomic resolution on the $\alpha_3\beta_3\gamma$ complex (Abrahams et al., 1994). The catalytic site of F_1-ATPase resides on the β subunit (Abrahams et al., 1994; Senior, 1988; Futai et al., 1989). The subassembly $\alpha_3\beta_3$ forms a ring with long helices of the γ subunit in the center, hinting rotational catalysis. The tertiary structure of the β subunit in the F_1-ATPase differs according to the state of its active site, namely, an empty, Mg·AMP-PNP binding, or Mg·ADP binding state (Abrahams et al., 1994). The empty and nucleotide binding forms can be specified as the open and closed forms, respectively, because of their conformations. Recently, the rotation of the γ subunit in the fixed $\alpha_3\beta_3$ complex on hydrolysis of ATP has been directly demonstrated by epifluorescence microscopy for the $\alpha_3\beta_3\gamma$ complex from thermophilic bacillus PS-3 (TF_1) (Noji et al., 1997). These reports strongly support the cyclical binding change mechanism of ATP synthesis (Cross, 1981). To elucidate the binding change mechanism, the intrinsic conformational change in the β subunit induced by the nucleotide binding and the interactions among the α, β, and γ subunits should be carefully investigated in connection with the mechanism of rotation and catalysis. We would like to ask in this work if the conformational change from the open to closed forms can be induced even in the absence of α and γ subunits, namely, in the monomer β subunit. This is important to an understanding of the driving forces of the conformational change in the F_1-ATPase.

Although the β monomer has no ATPase activity, the dissociation constant of the β-ATP complex (15 μM; Odaka et al., 1994) is similar to K_{d3} of the F_1-ATP complex (25 μM: Weber et al., 1994). Therefore, the structure of the substrate binding site should be similar for the F_1 and β monomers. The TF_1 β subunit is suitable for the study of the conformation and function of the isolated β monomer because of its high stability. The crystal structure of the TF_1 nucleotide-free $\alpha_3\beta_3$ complex has been reported (Shirakihara et al., 1997). The structure of the β subunit of the complex is similar to that of MF_1-ATPase in the empty state (open form). Therefore, the major characteristics of the crystal structure of MF_1-ATPase should also be characteristics of TF_1-ATPase. The β subunit is roughly composed of three domains, namely, the amino (N-) terminal, nucleotide-binding, and carboxyl (C-) terminal domains (Fig. 1). Because tyrosine (Tyr) residues are scattered all over the TF_1 β subunit as shown in Fig. 1, we focused our attention on the Tyr residues to examine the effect of the nucleotide binding on the structure. In the TF_1 β subunit, there are 12 Tyr residues, of which Tyr^{277}, Tyr^{307}, Tyr^{341}, and Tyr^{364} (*underlined* in Fig. 1) are conserved in the primary sequences of the β subunits of all known F_1-ATPase. The roles of the conserved residues are not yet well understood.

Received for publication 5 January 1999 and in final form 10 June 1999.

Address reprint requests to Dr. Hideo Akutsu, Department of Chemistry and Biotechnology, Faculty of Engineering, Yokohama National University, Hodogaya-ku, Yokohama 240-8501, Japan. Tel.: +81-45-339-4232; Fax: +81-45-339-4251; E-mail: akutsu@ynu.ac.jp.

Dr. Tozawa's present address is Faculty of Integrated Arts and Sciences, The University of Tokushima, 1-1 Minamijosanjima-cho, Tokushima 770-8502, Japan.

0006-3495/99/10/2175/09 $2.00

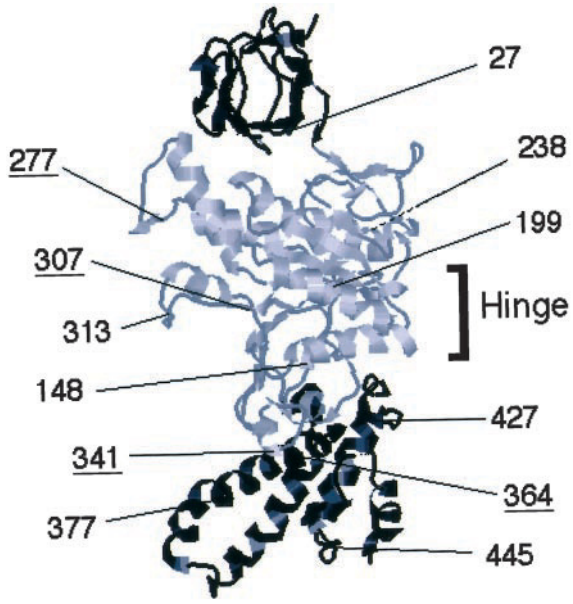

FIGURE 1 The locations of 12 tyrosine residues in the TF_1 β subunit (Shirakihara et al., 1997). Sequence numbers are presented for the Tyr residues. Conserved residues are underlined. The N-terminal, nucleotide-binding, and C-terminal domains are drawn in different shades of gray from the top to the bottom. The hinge region responsible for the conformational change between the open and closed forms is indicated on the right.

To obtain the conformational and functional information, a combination of ^{1}H-NMR and mutagenesis of the β subunit and ATPase activity examination of the reconstituted $\alpha_3\beta_3\gamma$ complex were employed in this work. The aromatic proton resonances from all 12 tyrosine residues were identified and assigned using site-directed mutagenesis. We observed a well-defined conformational change in the β subunit with the binding of nucleotide to the β monomer.

MATERIALS AND METHODS

Materials, bacterial strains, and growth media

Deuterium oxide (99.9 and 99.96 atom %^{2}H) was purchased from ISOTEC and Showadenko. Sulfuric acid-d_2 (99.3 atom% ^{2}H) and L-4-hydroxyphenyl-2,6-d_2-alanine (L-tyrosine, 98 atom% ^{2}H) were purchased from ISOTEC, and deuterium chloride (99.5 atom% ^{2}H) was from Cambridge Isotope Laboratories. 5′-Adenylylimidodiphosphate (AMP-PNP) and *N*-(phosphonomethyl)-glycine (glyphosate) were obtained from Sigma. Restriction enzymes, T4 DNA ligase, T4 polynucleotide kinase, and DNA polymerase were purchased from Takara. The oligonucleotides used for introducing mutation were obtained from Takara. Other chemicals were in analytical grade. *Escherichia coli* strain HB101 (*supE*44, *hsdS*20(*r*B-*m*B-), *recA*13, *ara*-14, *proA*2, *lacY*1, *galK*2, *rpsL*20, *xyl*-5, *mtl*-1, *leuB*6, *thi*-1) and DK8 (*bglR*, *thi*-1, *rel*-1, HfrPO1, Δ(*uncB-uncC*) *ilv*::Tn10) were used for the production of the wild-type and mutant TF_1-β subunits, respectively. Other strains used for the generation of oligonucleotide-directed mutants and the production of α and γ subunits were described previously (Yohda et al., 1988; Tozawa et al., 1992). For preparation of the selectively deuterated subunit, cells were grown on a nutrient-rich medium in test tubes and subsequently on a minimal medium supplemented with glyphosate and a mixture of amino acids resembling the composition of casamino acids at 37°C, with vigorous shaking (Matthews et al., 1977). Glyphosate, an inhibitor of aromatic amino acid biosynthesis, was added to the culture medium to facilitate the incorporation of the aromatic amino acids (Kim et al., 1990). L-Phenylalanine, L-histidine, and L-tyrosine were replaced by L-[2,3,4,5,6-^{2}H]phenylalanine, DL-[α,2,4-^{2}H]histidine, and L-[2,6-^{2}H]tyrosine, respectively, for the specific deuteration of the β subunit. In other cases, cells were grown on a nutrient-rich medium at 37°C with vigorous shaking.

Selective deuteration of amino acids

L-[2,3,4,5,6-^{2}H]Phenylalanine was prepared according to the method of Matthews et al. (1977). DL-[α,2,4-^{2}H]Histidine was prepared as follows. L-Histidine was dissolved in 6 N ^{2}HCl and placed in an ample tube. The tube was sealed, placed in a stainless steel portable reactor, and heated at 190°C for 2 h in an oven. The cooled reaction mixture was decolorized with active carbon. After evaporation, the histidine was dissolved in a small amount of H_2O and then recrystallized by adding 10 volumes of ethanol and cooling gradually to 4°C. Then, the C-2 protons were further deuterated: under an N_2 atmosphere, ^2H_2O was added to the histidine and the p^{2}H was adjusted to 8–9 with NaO^{2}H. The solution was refluxed under nitrogen flow at 80°C for 48 h, followed by crystallization at pH 3.36. The extent of deuteration was confirmed by ^{1}H-NMR.

NMR measurements

The wild-type and mutant β subunits of TF_1 expressed in *E. coli* were purified as described previously (Yohda et al., 1988; Ohtsubo et al., 1987). The exchangeable protons of the protein sample for NMR measurements were replaced with deuterons by repeated cycles of lyophilization. At the final step, the sample was dissolved in a 50 mM sodium phosphate ^2H_2O buffer, p^{2}H 7.8, at 0.25–1 mM protein concentration. The pH meter readings were not corrected for the deuterium isotope effect. Chemical shifts are referred to an internal standard of sodium 2,2-dimethyl-2-silapentane-5-sulfonate (DSS). It was confirmed that the ^{1}H-NMR spectrum of the β subunit in phosphate buffer is identical with that in Tris-^{2}HCl buffer. For ligand titration, a small amount of a concentrated ligand solution was added directly to the sample solution. Preparation of a Mg·nucleotide solution was as follows: equimolar amounts of nucleotide and $MgCl_2$ were dissolved in deuterium oxide. This mixture was lyophilized several times, then dissolved in a 50 mM sodium phosphate buffer (p^{2}H 7.8) at an appropriate concentration. The addition of the ligand solution did not affect the p^{2}H of the NMR sample solution, which was confirmed after the titration experiment. ^{1}H-NMR spectra were recorded at 400 MHz on a Bruker DRX400 NMR spectrometer.

Other methods

Mutated TF_1 β subunit genes were obtained by oligonucleotide-directed mutagenesis (Kunkel et al., 1987). Reconstitution of the $\alpha_3\beta_3\gamma$ complex from the α, β, and γ subunits and assay of its ATPase activity were carried out as described previously (Tozawa et al., 1992; Miwa and Yoshida, 1989). Protein concentration was determined by the method of Bradford (1976), using bovine serum albumin as a standard. The molecular weight of the TF_1 β subunit was examined by high-performance liquid chromatography (Gilson) with a column of TSK-GEL G-3000.

RESULTS

Simplification of the ^{1}H-NMR spectrum of the TF_1 β subunit

Fig. 2 *A* is the aromatic region of a ^{1}H-NMR spectrum of the TF_1 β subunit. Because this region includes the signals from 157 protons of 17 phenylalanine (Phe), 12 histidine (His),

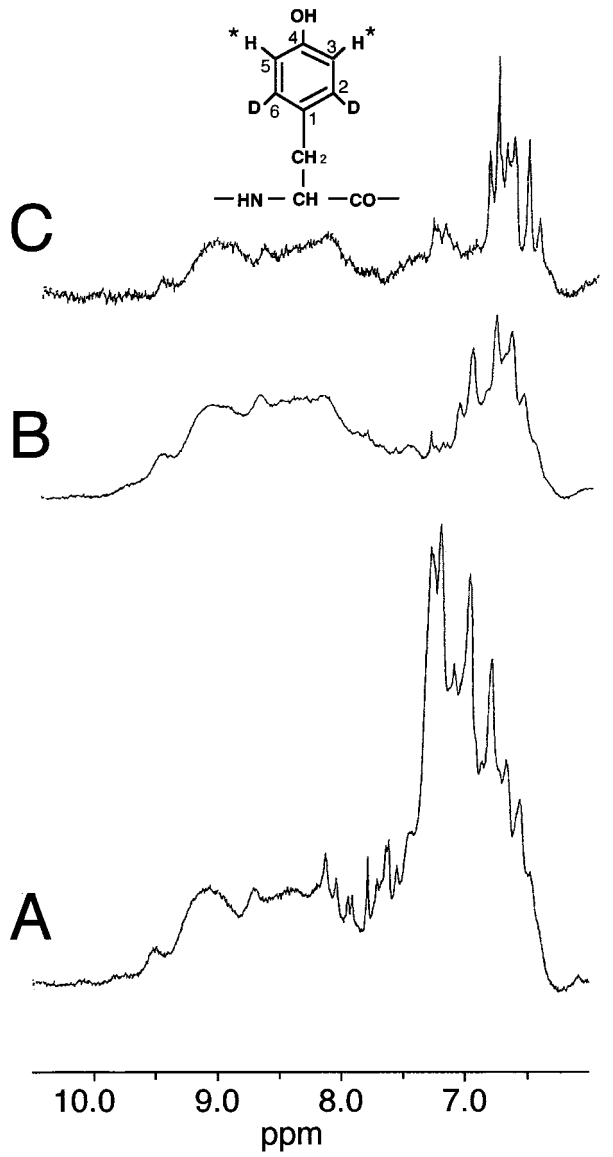

FIGURE 2 ^{1}H-NMR spectra of the wild-type TF_1 β subunit at p^{2}H 7.8 and 30°C. (*A*) The nonlabeled β subunit. (*B*) The β subunit specifically deuterated with [2,3,4,5,6-^{2}H]phenylalanine and [α,2,4-^{2}H]histidine ([^{2}H-F, H]β). (*C*) The protein specifically deuterated with [2,3,4,5,6-^{2}H]phenylalanine, [α,2,4-^{2}H]histidine, and [2,6-^{2}H]tyrosine ([^{2}H-F, H, Y]β). The residual protons of the tyrosine residue are shown in the chemical structure at the top.

and 12 tyrosine (Tyr) residues, well-resolved signals could not be obtained, except for some signals due to histidyl C2 protons (Tozawa et al., 1995). To obtain the information on the tyrosine residues, the spectrum was simplified extensively by means of incorporation of the deuterated aromatic amino acids. On the incorporation of His and Phe fully deuterated in the rings ([^{2}H-F, H]β), most protons from 17 Phe and 12 His residues were eliminated (Fig. 2 *B*). Because TF_1 β has no tryptophan residue, the remaining resonances in this region should be attributed to the tyrosine residues and peptide amide groups. The additional incorporation of L-[2,6-^{2}H]Tyr ([^{2}H-F, H, Y]β) further simplified the spectrum (Fig. 2 *C*). Moreover, significant narrowing of the Tyr resonances was achieved by the elimination of the dipole-dipole interactions between the vicinal protons in the ring. Now, 10 separate peaks can be observed. These signals can be used to probe the microenvironment of the Tyr residues in the β subunit.

Resonance assignment of 3,5-aromatic ring protons of tyrosine residues

Twelve mutant proteins, in each of which a Tyr residue had been replaced by a Phe by site-directed mutagenesis, were prepared for the assignment of the residual aromatic proton resonances of Fig. 2 *C*. The spectra of the mutant proteins in the aromatic region are summarized in Fig. 3. The spectra were measured at 40°C for better resolution. Here, βY313F, for example, stands for a mutant β subunit in which Tyr^{313} is replaced by Phe. Fortunately, substitutions only affected the signals of the substituted Tyr. For instance, the spectrum of βY148F lacks peak 5 at 6.72 ppm, indicating that the

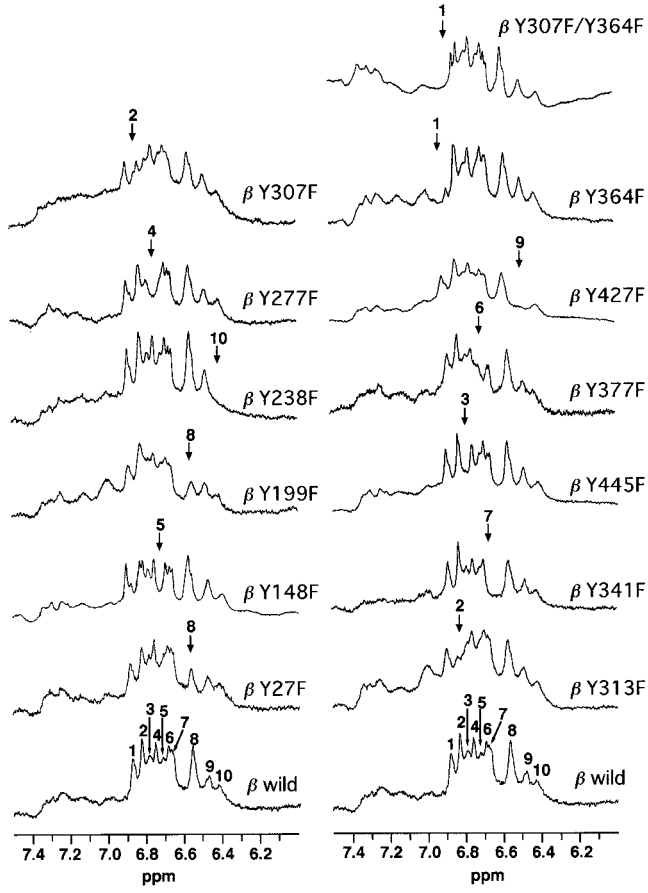

FIGURE 3 ^{1}H-NMR spectra of the TF_1 [^{2}H-F, H, Y]β subunits of wild type and 13 mutants in the aromatic region at p^{2}H 7.8 and 40°C. See the caption of Fig. 2 for [^{2}H-F, H, Y]β. The mutated site is indicated on the right. βY27F, for instance, stands for the β subunit, in which Tyr^{27} is replaced by phenylalanine. The arrows indicate the positions of the disappeared signals. In the case of βY307F/Y364F, the arrow indicates the peak confirmed only by the double mutant.

resonance can be ascribed to Tyr^{148}. The intensity of peak 8 is significantly weakened in the spectrum of βY27F, suggesting that the peak includes the resonance due to Tyr^{27}. All other resonances were assigned in a similar way. However, a small signal at peak 1 of the βY364F spectrum was left unassigned. This signal could be assigned to Tyr^{307} by using a double mutant of βY307F/Y364F, as can be seen in the spectrum on the top of Fig. 3. All intensity of peak 1 disappeared in this spectrum. This means that Tyr^{307} gives rise to two peaks. The assignment is summarized in Table 1. In addition to peak 1, the resonances of Tyr^{307} and Tyr^{313} overlap at 6.83 ppm (peak 2), and the resonances of Tyr^{27} and Tyr^{199} overlap at 6.56 ppm (peak 8).

The resonances of Tyr^{307}, Tyr^{313}, and Tyr^{341} are observed as doublets. Either the flip-flop motion of the ring is suppressed by the rigid environment or there are two conformations exchanging at a slow rate. The presence of two conformations in a helix along the conical tunnel was reported on the basis of the C2 proton signal of His^{200} in the β monomer (Tozawa et al., 1995).

Ligand titration of the [^{2}H-H, F, Y]β spectrum

To examine the effect of the nucleotide binding on the Tyr residues at various positions, ligand titration experiments were carried out. As can be seen in Fig. 4, the addition of a ligand Mg·ATP or Mg·AMP-PNP induces a change in the spectrum of the [^{2}H-H, F, Y]β subunit. Although the characteristic features of the change are similar for Mg·ATP and Mg·AMP-PNP, the extent of the change is definitely smaller for Mg·AMP-PNP than that for Mg·ATP, suggesting that the dissociation constants are different for these two ligands. In both cases, however, the significant change was restricted to the signals of Tyr^{148} (×), Tyr^{238} (*filled squares*), Tyr^{341} (*filled circles*), one of peak 1 (*empty circles*), and one of peak 8 (*empty squares*). The change in the chemical shift of Tyr^{341} was the most significant among them. The crystal structure of MF_1 showed that the aromatic ring of this residue is almost stacked to the adenine ring of AMP-PNP (Abrahams et al., 1994). The upfield shift suggests that the adenine ring of the ligand and the aromatic ring of the tyrosine are actually stacked on each other in the isolated β subunit as well. It has been reported on the basis of chemical modification and mutation experiments that this Tyr residue is involved in the nucleotide binding (Odaka et al., 1994; Bullough and Allison, 1986; Garin et al., 1986; Cross et al., 1987; Admon and Hammes, 1987; Weber et al., 1993, 1994). Our result has provided the evidence for the role of this residue in the nucleotide binding in the monomer. A conformational change affecting Tyr^{341}, however, is not completely excluded.

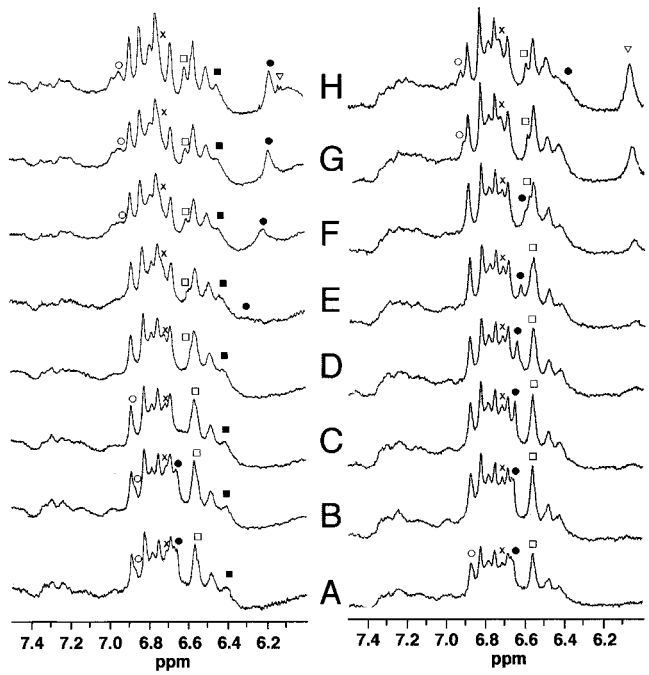

FIGURE 4 Titration of the tyrosine resonances of the TF_1 [^{2}H-F, H, Y]β subunit by the adenine nucleotide at p^{2}H 7.8 and 40°C. (*Left*) Titrated by Mg·ATP. (*Right*) Titrated by Mg·AMP-PNP. The concentration ratios of the nucleotide to protein are 0, 0.01, 0.1, 0.2, 0.5, 1.0, 2.0, and 3.0 for *A*, *B*, *C*, *D*, *E*, *F*, *G*, and *H*, respectively. The protein concentration is 0.5 mM. ×, Tyr^{148}; □, Tyr^{199}; ■, Tyr^{238}; ○, Tyr^{307}; ●, Tyr^{341}; ▽, C1′ proton of ribose of the nucleotide. See the caption of Fig. 2 for [^{2}H-F, H, Y]β.

TABLE 1 Assignment of the 3,5 ring proton resonances of the tyrosine residues in the wild-type β subunit at p^{2}H 7.8 and 40°C

Signal no.	Chemical shift (ppm)	Tyr no.
1	6.87	307
	6.88	364
2	6.83	307
		313
3	6.79	445
4	6.75	277
5	6.72	148
6	6.69	377
7	6.67	341
8	6.56	27
		199
9	6.48	427
10	6.43	238

Signal numbers are given at the bottom of Fig. 2.

One resonance of peak 8 (Tyr^{27} and Tyr^{199}) moved to a lower field on binding of the ligand. Because this downfield shift could not be observed in βY199F, the shifted signal can be assigned to Tyr^{199}. The shifted signal of peak 1 was assigned to Tyr^{307} by the titration experiment on βY364F, which gives the isolated Tyr^{307} signal. This was further confirmed using a double mutant protein βY313F/Y364F (Fig. 5). The chemical shift changes of the relevant tyrosine residues for the nucleotide-bound forms are summarized in Table 2. The signals of Tyr^{144}, Tyr^{199}, Tyr^{238}, and Tyr^{307} shifted downfield. In contrast to Tyr^{341}, these residues are not in the binding site but scattered in the central domain in view of the MF_1 ATPase and TF_1 $\alpha_3\beta_3$ crystal structures, showing that the binding of Mg·ATP induces a conforma-

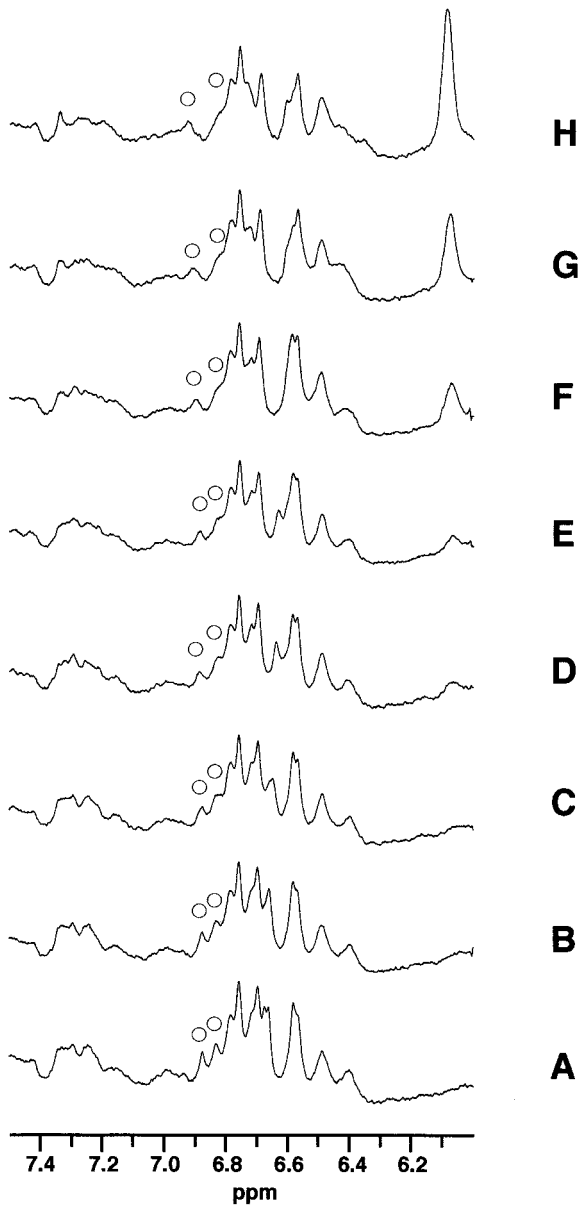

FIGURE 5 Titration of the tyrosine resonances of the TF_1 [^{2}H-F, H, Y]βY313F/Y364F subunit by Mg·AMP-PNP at p^{2}H 7.8 and 40°C. The concentration ratios of the nucleotide to protein are 0, 0.1, 0.2, 0.5, 1.0, 2.0, 3.0, and 5.0 for *A*, *B*, *C*, *D*, *E*, *F*, *G*, and *H*, respectively. The protein concentration is 0.5 mM. ○, Tyr^{307}. See the caption of Fig. 2 for [^{2}H-F, H, Y]β.

tional change only in the central domain of the β subunit. In the spectrum of the double mutant protein βY313F/Y364F, we can see the doublet of Y307 directly. With the addition of Mg·AMP-PNP, only the signal at a lower field shifted significantly, as shown in Fig. 5.

The chemical shift is plotted in Fig. 6 as a function of the ratio of ligand to protein for Mg·AMP-PNP and Mg·ATP. To confirm the resonance assignment of Tyr^{341} in Figs. 4 and 6, the effect of Mg·ATP on the βY341F was also examined. No resonance shifted upfield with the addition of the ligand, supporting the assignment. A discontinuous change was observed with the addition of Mg·ATP (Fig. 4, *left*). This was verified as follows. Fig. 6 shows that the chemical shift of the bound form for Mg·ATP is 6.17 ppm, and the binding stoichiometry is 1:1. At a ligand/protein ratio of 0.5, however, the signal appeared at ~6.3 ppm. Because this chemical shift is much closer to that of the bound form than that of the free form (6.67 ppm), this signal can be ascribed to the bound form in the discontinuous shift. This corresponds to an intermediate slow exchange. Because the sharpest signal of the bound form was obtained for ATP·β complex, the exchange rate was estimated by using the chemical shift of this signal at ATP/protein = 0.5 (6.26 ppm). Under an intermediate slow exchange between the two conformers at a ratio of 1:1, the relationship

$$(\nu_f - \nu_b)/(\nu_{fo} - \nu_{bo}) = [1 - 1/2\pi^2\tau^2(\nu_{fo} - \nu_{bo})^2]^{1/2} \quad (1)$$

can be obtained, where ν_f, ν_b, ν_{fo}, ν_{bo}, and τ are, respectively, the resonance frequencies of the signals of the free and bound forms with and without exchange and the exchange time (Pople et al., 1959). The exchange rate obtained was 6.8×10^2 s^{-1}, provided that most ATP are bound to the β subunits and $\nu_{fo} - \nu_f = \nu_b - \nu_{bo}$. Judging from the broadening of the signal, the exchange rates for different ligands are on the order of ATP < Mg·ATP < ADP < Mg·ADP.

A successive upfield shift of the Tyr^{341} signal occurred with the addition of Mg·AMP-PNP, as can be seen in Fig. 4 (*right*) and Fig. 6. It suggests that the exchange rate is much faster than 7×10^2 s^{-1} in view of the slow exchange rate obtained above. This was also the case with Mg·AMP. The dissociation constants (K_d) of Mg·AMP-PNP were estimated by nonlinear least-squares fitting to the data in Fig. 6. The best-fit K_d and limiting shift for the bound form were $(9.6 \pm 0.4) \times 10^2$ μM and 6.13 ppm, respectively. The binding stoichiometry was 1:1, as in the case of the Mg·ATP·β complex. This is consistent with the binding stoichiometry in the F_1-ATPase. The K_d value for Mg-AMP was estimated using 6.17 ppm as the chemical shift of the bound form; this was 4×10^4 μM. The K_d values for Mg·ATP, ATP, Mg·ADP, and ADP were reported to be 15, 15, 11, and 8.5 μM, respectively (Odaka et al., 1994; Ohta et al., 1980). Therefore, the dissociation constant changes drastically between AMP and ADP.

The spectra at a ligand/protein ratio of 3.0 are compared for Mg·AMP, Mg·ADP, ADP, ATP, Mg·ATP, and Mg·AMP-PNP in Fig. 7. The chemical shift changes of the relevant tyrosine residues are included in Table 2. Although the addition of Mg·ADP also induced a similar effect on the spectrum, the signals of Tyr^{199} (*empty squares*) and Tyr^{307} at 6.88 ppm (*empty circles*) were not affected significantly, and the Tyr^{238} (*filled squares*) signal did not shift at all. This means that Mg·ADP induces a change in the β subunit that is distinctly different from that induced by Mg·ATP. Mg·AMP-PNP induces a change similar to that induced by Mg·ATP, although the dissociation constant is different. In contrast, the spectra of ATP·β and ADP·β subunit com-

TABLE 2 Chemical shift changes of the relevant tyrosine (Y) residues of the nucleotide-bound β subunit in comparison with the free one

	Y307	Y148	Y341	Y199	Y238
Nucleotide	6.87	6.72	6.67	6.56	6.43 ppm
Mg · ATP	0.07	0.02	−0.50	0.04	0.02 ppm
(Mg · AMP-PNP	0.07	0.02	−0.44	0.04	0.02)
ATP	0.01	0.02	−0.50	0.04	0.00
Mg · ADP	0.01	0.02	−0.50	0.02	0.00
ADP	0.01	0.02	−0.50	0.02	0.00
(Mg · AMP	0.00	0.00	−0.03	0.00	0.00)

The concentration ratio of nucleotide to protein is 3.0 except for Mg · AMP-PNP. The ratio of the latter is 8.0. The data for Mg · AMP-PNP and Mg · AMP are not for the fully ligand bound β subunit. The chemical shifts for the free β subunit are shown on the top.

plexes are distinctly different from that of the Mg·ATP·β complex but similar to that of the Mg·ADP·β complex. This fact clearly shows the different role of Mg^{2+} in nucleotide·β complex formation for ATP and ADP.

Effects of amino acid substitutions on the ATPase activity of the reconstituted $\alpha_3\beta_3\gamma$ complexes

To examine the role of each tyrosine residue, the mutant β subunits were reconstituted into the $\alpha_3\beta_3\gamma$ complexes, and their ATPase activities were examined. The results are summarized in Table 3. The results can be classified into three groups. The first is mutations that did not affect the ATPase activity significantly. The second is mutations that suppressed the activity significantly. The third mutation eliminated the ability to form the complex. βY307F and βY445F can be placed in the second category, βY277F in the third, and the rest of them in the first one. The chemical modification and mutation of Tyr^{307} have been extensively investigated (Parsonage et al., 1987; Yoshida and Allison, 1990, and the references therein). In contrast, the importance of the conserved Tyr^{277} is reported for the first time in this work.

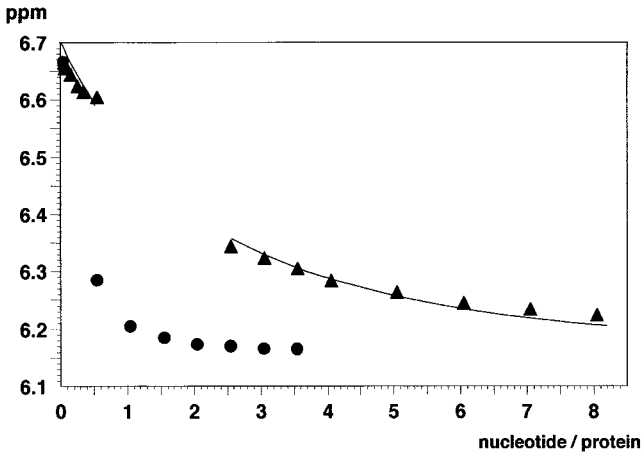

FIGURE 6 Titration curves of the Tyr^{341} signals as a function of the nucleotide/protein ratio. ●, Mg·ATP; ▲, Mg·AMP-PNP. The protein concentration is 0.5 mM. The solid line is the best-fit curve obtained by nonlinear least-squares fitting.

DISCUSSION

The assignment of the 3,5 ring proton signals of all Tyr residues brings a new insight into the β subunit-nucleotide interactions. The signals of Tyr^{148}, Tyr^{199}, Tyr^{238}, and Tyr^{307} have shifted downfield with the binding of Mg·ATP or Mg·AMP-PNP. All of them are located in the nucleotide binding domain, especially in the hinge region (Fig. 1). Furthermore, the chemical shift of the C-2 ring proton of His^{200} was also found to change when Mg·AMP-PNP interacted with the isolated $TF_1\beta$ (Tozawa et al., 1995). Therefore, it can be concluded that the local conformation in the hinge region changes with nucleotide binding, whereas most of the other part is not significantly affected. Actually, this is the situation found in the crystal structure of MF_1. The relative orientations of the N- and C-terminal domains of the β subunit differ for the empty state (open form) and the nucleotide binding state (closed form). The conformational variation in the two forms originates in the different angles of the hinges in the nucleotide binding domains (Abrahams et al., 1994). The β strand including Tyr^{307} (from Ile^{306} to Val^{308}) in the nucleotide-binding state is disrupted in the empty state. The mapping of the Tyr residues that underwent the chemical shift changes on the β subunit structure fall in the region showing the conformational variation between the open and closed forms in the crystal structure of MF_1. Because the nucleotide-free β monomer takes the open form in the crystal structure (Kita et al., 1996), the nucleotide binding to the isolated β subunit should induce a conformational change from the open to the closed form. This conclusion suggests that the conformational change between the open and closed forms is directly associated with binding of the nucleotide, even in the free β subunit. This intrinsic conformational change in the β subunit induced by the nucleotide binding may be one of the essential driving forces for the F_1 rotation.

Furthermore, the conformation of the nucleotide-bound β subunit differs for Mg·ATP and Mg·ADP, as shown by the signals of Tyr^{199}, Tyr^{238}, and Tyr^{307} at 6.87 ppm. It is now

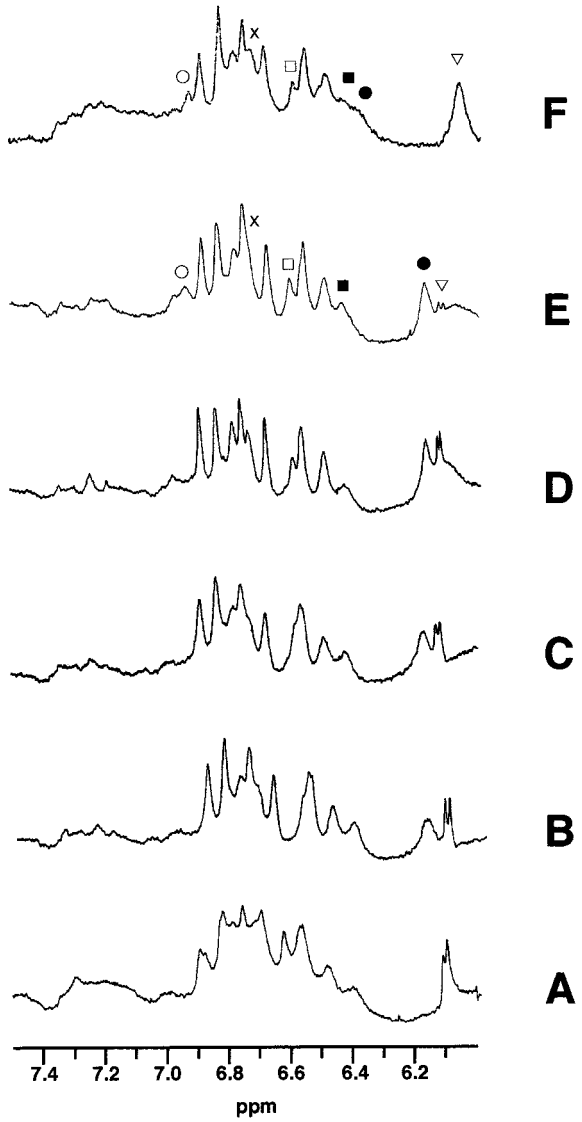

FIGURE 7 The aromatic regions of the ^{1}H-NMR spectra of the TF_1 [^{2}H-F, H, Y]β subunit in the presence of different nucleotides at p^{2}H 7.8 and 40°C. (*A*) Mg·AMP. (*B*) ADP. (*C*) Mg·ADP. (*D*) ATP. (*E*) Mg·ATP. (*F*) Mg·AMP-PNP. The concentration ratio of the nucleotide to protein is 3.0. ×, Tyr^{148}; □, Tyr^{199}; ■, Tyr^{238}; ○, Tyr^{307}; ●, Tyr^{341}; ▼, C1′ proton of ribose of the nucleotide. See the caption of Fig. 2 for [^{2}H-F, H, Y]β.

well established that the binding of Mg·ATP induces the rotation of F_1, resulting in the hydrolysis of ATP (Noji et al., 1997). Mg·ADP, however, leads F_1 to the Mg·ADP inhibited form. These observations are consistent with the different conformations found for the Mg·ATP·β and Mg·ADP·β monomer complexes. It is known that ATP is hardly hydrolyzed by EF_1-ATPase in the absence of Mg^{2+} (Weber et al., 1994, 1998). Our result has shown that the isolated β subunit binding with ATP takes on the conformation similar to that with Mg·ADP rather than that with Mg·ATP. This would explain the abortive ATPase activity of EF_1 (F_1-ATPase from *E. coli*) in the absence of Mg^{2+}.

The exchange rate and dissociation constant change drastically from AMP to ADP, but do not from ADP to ATP.

TABLE 3 ATPase activity of the reconstituted $\alpha_3\beta_3\gamma$ complex

Mutant β in $\alpha_3\beta(\text{mutant})_3\gamma$	Activity of the complex	
	unit/mg protein	%
Wild	6.0	100
Y27F	2.8	47
Y148F	3.1	52
Y199F	6.0	100
Y238F	3.2	54
Y277F	X	X
Y307F	1.5	25
Y313F	16.3	272
Y341F	7.7	128
Y364F	13.4	223
Y377F	5.5	92
Y427F	3.6	60
Y445F	1.5	25

One unit is the activity that hydrolyzes 1 μmol of ATP/min at 25°C. A mutant Y27F, for example, stands for the β subunit, in which Tyr^{27} is replaced by phenylalanine.
X, the $\alpha_3\beta_3\gamma$ complex was not formed.

Even the presence of Mg^{2+} does not affect the dissociation constant significantly. This strongly suggests that one of the major factors in the nucleotide binding is the interaction between the β-phosphate and polypeptide. The P loop region was indicated to be responsible for the phosphate binding (Milburn et al., 1990; Story and Steitz, 1992; Abrahams et al., 1994). Close inspection of the two and three nucleotide binding sites of the β and α subunits, respectively, of the MF_1 crystal structure (Abrahams et al., 1994) was carried out. Most amide groups in the P loop region seem to be involved in the hydrogen bonding with the nucleotide phosphates, as shown in Table 4. Six out of eight pairs at short distances are involved in the interactions with the β-phosphate, confirming the important role of the β-phosphate in nucleotide binding. In the case of a natural ligand, namely, Mg·ADP, three strong hydrogen bonds including the shortest one are formed with the β-phosphate.

Only the functional role of Tyr^{277} in the conserved four tyrosine residues has never been discussed. The mutant βY277F was found not to form the complex with α and γ subunits. Tyr^{277} is located in a large loop (Fig. 1), which forms the "hydrophobic sleeve" that is in close contact with the C-terminal helix of the γ subunit together with the corresponding loops of three α subunits in the crystal structure of MF_1 ATPase (Abrahams et al., 1994). The side chain of Tyr^{277} forms a hydrogen bond with the carboxyl group of aspartic acid $(Asp)^{315}$, which is located in a different loop in the proximity (indicated by Tyr^{313} in Fig. 1) of the all β subunits of the MF_1 structure. This loop was assumed by Abrahams et al. to be one of the catch regions. A mutant protein of βQ304C was also unable to form the $\alpha_3\beta_3\gamma$ complex (Yoshida et al., unpublished data). In the crystal structure, glutamine $(Gln)^{304}$ is located in a β strand connected to the loop including Asp^{315}. Gln^{304} forms a hydrogen bond with Gln^{289}, which is located in a helix connected to the loop including Tyr^{277}. This hydrogen bond would not

TABLE 4 The distances (Å) between the amide nitrogen and phosphate oxygen found in the crystal structure of MF_1 (Abrahams et al., 1994)

Amide/phosphate	αO1	αO3	βO1	βO2	βN(O)3	γO1
α-172, β-159					2.93 ± 0.28 (2.65)	2.83 ± 0.30
α-173, β-160			3.12 ± 0.45 (3.32)			
α-174, β-161		2.97 ± 0.30 (3.27)	3.07 ± 0.32 (2.88)			
α-175, β-162			2.91 ± 0.54 (2.50)			
α-176, β-163				3.11 ± 0.05 (3.13)		
α-177, β-164	2.88 ± 0.22 (3.02)					

Only the distances shorter than 3.5 Å are shown. αO3 and βN(O)3 bridge α and β, and β and γ phosphoruses, respectively. The relevant regions are Gln(172)-Thr-Gly-Lys-Thr-Ser(177) and Gly(159)-Val-Gly-Lys-Thr-Val(164) for the α and β subunits, respectively. Five data were averaged except for γO1, for which four data were averaged. In the case of βN3, the length for βO3 in the β-ADP complex (β_{DP}) is also included. The values for β_{DP} are shown in parentheses.

be formed in βQ304C because of the shorter side chain of cysteine, suggesting that this hydrogen bond is essential to complex formation. Thus the two hydrogen bonds between Tyr^{277} and Asp^{315} and between Gln^{289} and Gln^{304} would be essential to the stabilization of the hydrophobic sleeve and catch structure in the $\alpha_3\beta_3\gamma$ complex. The four residues mentioned above are conserved in all known β subunits.

In conclusion, ^{1}H-NMR results have shown a conformational change in the isolated TF_1 β subunit similar to that found in the crystal structure of MF_1-ATPase with the binding of nucleotides. The mode of the conformational change differs for Mg·ATP and Mg·ADP. This kind of intrinsic conformational change would work as one of the driving forces of the rotation of F_1-ATPase. Tyr^{341} is directly involved in the nucleotide binding in the β subunit monomer through stacking with the adenine ring. Furthermore, the conserved Tyr^{277} was found to be essential to the formation of the $\alpha_3\beta_3\gamma$ complex, presumably by stabilization of the hydrophobic sleeve and catch structure.

We are grateful to Prof. M. Kainosho (Tokyo Metropolitan University) for his kind instruction on the deuteration of histidine and phenylalanine.

This work was partly supported by a grant in aid (no. 09480173) from the Ministry of Education, Science and Culture of Japan (HA), the Proposal Base Advanced Industrial Technology R&D Program from the New Energy and Industrial Technology Development Organization of Japan (HA), and a fellowship from the Japan Society for the Promotion of Science (KT and HY).

REFERENCES

Abrahams, J. P., A. G. W. Leslie, R. Lutter, and J. E. Walker. 1994. Structure at 2.8 Å resolution of F_1-ATPase from bovine heart mitochondria. *Nature.* 370:621–628.

Admon, A., and G. Hammes. 1987. Amino acid sequence of the nucleotide binding region of chloroplast coupling factor 1. *Biochemistry.* 26: 3193–3197.

Bradford, M. M. 1976. A rapid and sensitive method for the quantitation of microgram quantities of protein utilizing the principle of protein-dye binding. *Anal. Biochem.* 72:248–254.

Bullough, D. A., and W. S. Allison. 1986. Inactivation of the bovine heart mitochondrial F_1-ATPase by 5′-*p*-fluorosulfonylbenzoyl[^{3}H]inosine is accompanied by modification of tyrosine 345 in a single β subunit. *J. Biol. Chem.* 261:14171–14177.

Cross, R. L. 1981. The mechanism and regulation of ATP synthesis by F_1-ATPases. *Annu. Rev. Biochem.* 50:681–714.

Cross, R. L., D. Cunningham, C. G. Miller, Z. Xue, J. M. Shou, and P. D. Boyer. 1987. Adenine nucleotide binding sites on beef heart F_1 ATPase: photoaffinity labeling of β-subunit Tyr-368 at a noncatalytic site and β Tyr-345 at a catalytic site. *Proc. Natl. Acad. Sci. USA.* 84:5715–5719.

Futai, M., T. Noumi, and M. Maeda. 1989. ATP synthase (H^+-ATPase): results by combined biochemical and molecular biological approaches. *Annu. Rev. Biochem.* 58:111–136.

Garin, J., F. Boulay, J. P. Issartel, J. Lunardi, and P. V. Viganais. 1986. Identification of amino acid residues photolabeled with 2-azido[α^{32}P]adenosine diphosphate in the β subunit of beef heart mitochondrial F_1-ATPase. *Biochemistry.* 25:4431–4437.

Kim, H.-W., J. A. Perez, S. J. Ferguson, and I. D. Campbell. 1990. The specific incorporation of labelled aromatic amino acids into proteins through growth of bacteria in the presence of glyphosate. Application to fluorotryptophan labelling to the H^+-ATPase of *Escherichia coli* and NMR studies. *FEBS Lett.* 272:34–36.

Kita, A., D. Xu, K. Kagitani, K. Saika, T. Matsui, M. Yoshida, and K. Miki. 1996. Crystallographic refinement of mutant β subunit of F_1-ATPase from thermophilic Bacillus PS3. *In* Proceedings of the Annual Meeting of the Crystallography Society of Japan. 120.

Kunkel, T. A., D. Robert, and R. A. Zakour. 1987. Rapid and efficient site-specific mutagenesis without phenotypic selection. *Methods Enzymol.* 154:367–382.

Matthews, H. R., K. S. Matthews, and S. J. Opella. 1977. Selectively deuterated amino acid analogues. Synthesis, incorporation into proteins and NMR properties. *Biochim. Biophys. Acta.* 497:1–13.

Milburn, M. V., L. Tong, A. M. DeVos, A. Brünger, Z. Yamaizumi, S. Nishimura, and S.-H. Kim. 1990. Molecular switch for signal transduction: structural differences between active and inactive forms of protooncogenic ras proteins. *Science.* 247:939–945.

Miwa, K., and M. Yoshida. 1989. The $\alpha_3\beta_3$ complex, the catalytic core of F_1-ATPase. *Proc. Natl. Acad. Sci. USA.* 86:6484–6487.

Noji, H., R. Yasuda, M. Yoshida, and K. Kinoshita. 1997. Direct observation of the rotation of F_1-ATPase. *Nature.* 389:299–302.

Odaka, M., C. Kaibara, T. Amano, T. Matsui, E. Muneyuki, K. Ogasahara, K. Yutani, and M. Yoshida. 1994. Tyr^{341} of the β subunit is a major K_m-determining residue of TF_1-ATPase: parallel effect of its mutations on K_d(ATP) of the β subunit and on K_m(ATP) of the $\alpha_3\beta_3\gamma$ complex. *J. Biochem.* 115:789–796.

Ohta, S., M. Tsuboi, T. Oshima, M. Yoshida, and Y. Kagawa. 1980. Nucleotide binding to isolated α and β subunits of proton translocating adenosine triphosphatase studied with circular dichroism. *J. Biochem.* 87:1609–1617.

Ohtsubo, M., M. Yoshida, S. Ohta, Y. Kagawa, M. Yohda, and T. Date. 1987. In vitro mutated β subunits from the F_1-ATPase of the thermophilic bacterium, PS3, containing glutamine in place of glutamic acid in positions 190 or 201 assembles with the α and γ subunits to produce inactive complexes. *Biochem. Biophys. Res. Commun.* 146:705–710.

Parsonage, D., S. Wilke-Mounts, and A. E. Senior. 1987. Directed mutagenesis of the β-subunit of F_1-ATPase from *Escherichia coli*. *J. Biol. Chem.* 262:8022–8026.

Pople, J. A., W. G. Schneider, and H. J. Bernstein. 1959. High-Resolution Nuclear Magnetic Resonance. McGraw-Hill, New York. 224.

Senior, A. E. 1988. ATP synthesis by oxidative phosphorylation. *Physiol. Rev.* 68:177–231.

Shirakihara, Y., A. G. W. Leslie, J. P. Abrahams, J. E. Walker, T. Ueda, Y. Sekimoto, M. Kambara, K. Saika, Y. Kagawa, and M. Yoshida. 1997. The crystal structure of the nucleotide-free $\alpha_3\beta_3$ subcomplex of F_1-ATPase from the thermophilic *Bacillus* PS3 is a symmetric trimer. *Structure.* 5:825–836.

Story, R. M., and T. A. Steitz. 1992. Structure of the recA protein-ADP complex. *Nature.* 355:374–376.

Tozawa, K., M. Odaka, T. Date, and M. Yoshida. 1992. Molecular dissection of the β subunit of F_1-ATPase into peptide fragments. *J. Biol. Chem.* 267:16484–16490.

Tozawa, K., N. Sekino, M. Soga, H. Yagi, M. Yoshia, and H. Akutsu. 1995. Conformational dynamics monitored by His-179 and His-200 of isolated thermophilic F_1-ATPase β subunit which reside at the entrance of the "conical tunnel" in holoenzyme. *FEBS Lett.* 376:190–194.

Weber, J., S. T. Hammond, S. Wilke-Mounts, and A. E. Senoir. 1998. Mg^{2+} coordination in catalytic sites of F_1-ATPase. *Biochemistry.* 37: 608–614.

Weber, J., S. Wilke-Mounts, R. S.-F. Lee, E. Grell, and A. E. Senior. 1993. Specific placement of tryptophan in the catalytic sites of *Escherichia coli* F_1-ATPase provides a direct probe of nucleotide binding: maximal ATP hydrolysis occurs with three sites occupied. *J. Biol. Chem.* 268: 20126–20133.

Weber, J., S. Wilke-Mounts, and A. E. Senior. 1994. Cooperativity and stoichiometry of substrate binding to the catalytic sites of *Escherichia coli* F_1-ATPase. *J. Biol. Chem.* 269:20462–20467.

Yohda, M., S. Ohta, T. Hisabori, and Y. Kagawa. 1988. Site-directed mutagenesis of stable adenosine triphosphate synthase. *Biochim. Biophys. Acta.* 933:156–164.

Yoshida, M., and W. S. Allison. 1990. The ATPase activity of the $\alpha_3\beta_3$ complex of the F_1-ATPase of the thermophilic bacterium PS3 is inactivated on modification of tyrosine 307 in a single β subunit by 7-chloro-4-nitrobenzofurazan. *J. Biol. Chem.* 265:2483–2487.